Research Paper

# Monitoring of three stages of paddy growth using multispectral vegetation index derived from UAV images

Samera Samsuddin Sah [a,b,e], Khairul Nizam Abdul Maulud [a,c,*], Suraya Sharil [a], Othman A. Karim [a], Biswajeet Pradhan [c,d]

[a] Department of Civil Engineering, Faculty of Engineering & Built Environment, Universiti Kebangsaan Malaysia, 43600 Bangi, Selangor, Malaysia
[b] Faculty of Civil Engineering & Technology, Universiti Malaysia Perlis, Kompleks Pusat Pengajian Jejawi 3, 02600 Arau, Perlis, Malaysia
[c] Earth Observation Centre, Institute of Climate Change, Universiti Kebangsaan Malaysia, 43600 Bangi, Selangor, Malaysia
[d] Centre for Advanced Modelling and Geospatial Information Systems (CAMGIS), School of Civil and Environmental Engineering, Faculty of Engineering and IT, University of Technology Sydney, Sydney, 2007 NSW, Australia
[e] Water Research and Environmental Sustainability Growth (WAREG), Center of Excellent (COE), Universiti Malaysia Perlis, 02600 Arau, Perlis, Malaysia

## ARTICLE INFO

## ABSTRACT

Paddy cultivation in Malaysia plays a crucial role in food production, with a focus on improving crop quality and quantity. With current national self-sufficiency levels ranging between 67 and 70%, the Malaysian government intends to produce higher-quality crops and boost agricultural production. However, the prominent paddy-producing state of Kedah has witnessed a decline in yields over the years. To address this, the study explores the effectiveness of unmanned aerial vehicles (UAVs) equipped with vegetation indices (VIs) for monitoring paddy plant health at various growth stages. Researchers acquired aerial imagery during two seasons in 2019, capturing three distinct growth stages: tillering (40 days after sowing), flowering (60 days after sowing), and ripening (100 days after sowing). These stages represent critical points in the paddy plant's life cycle. Agisoft Metashape software processed the images to extract VIs data. The study found that the Normalized Difference Vegetation Index (NDVI) and Blue Normalized Difference Vegetation Index (BNDVI) exhibited over 90% similarity. In contrast, the Normalized Difference Red Edge Index (NDRE), utilizing near-infrared and red-edge light reflections, demonstrated a unique relationship. NDRE outperformed NDVI and BNDVI with an R-squared value of 0.842, showcasing its superior accuracy, especially for dense crops like paddy plants sensitive to subtle changes in vegetation. In conclusion, this research highlights the potential of UAV-based VIs for effectively monitoring paddy plant health during different growth stages. The NDRE index, in particular, proves valuable for assessing dense crops, offering insights for precision agriculture and crop management in Malaysia.

## 1. Introduction

The eating of rice is synonymous with the Asian culture, including in Malaysia. According to Che Omar et al. (2019), Asian countries produced 495 million Metric Ton (MT) of rice in 2013. Southeast Asia contributes almost 40 % of the world's rice export, with Thailand, Vietnam, and Cambodia exporting the highest percentage of rice of 24.5%, 12.9%, and 1.3%, respectively. Malaysia is a rice importer, and in 2016, the country imported 2.2 % of the total world rice import (Che Omar et al., 2019; FAO, 2019). A total of ten granary areas in Malaysia are planted with paddy, and one of them is the Muda Agricultural

Development Authority (MADA) located in Kedah, a state in the North of Peninsular Malaysia. MADA contributes almost 40% of the nation's paddy production and is responsible for farm monitoring and providing advice and farm infrastructures to farmers. The MADA granary area covers the whole Kedah State, and some parts of Perlis State with a total planted area of up to 100 thousand hectares (Che Omar et al., 2019).

However, rice producing countries, including Malaysia, are faced with threat such as diseases (Abdul Hamid, 2018; Carneiro et al., 2019; Herman et al., 2015), water-related problems such as the water quality, sources, and irrigation system (Aboelsoud et al., 2022; Fikri Abdullah and Wan Mustapa, 2016; Gain et al., 2004; Mahmood et al., 2009; Ngoc

Thuy and Ha Anh, 2016; Rad et al., 2011; Sakaguchi et al., 2014; Shereen et al., 2005), and land scarcity (Amedie, 2013; Che Omar et al., 2019; Marfai, 2011) as well as the land fertility (Abdelrahman et al., 2022). The aforementioned paddy plant related threats have caused the country to suffer losses as a result of declining revenue.

Previously, paddy growth was monitored manually by the farmers (Sangeetha et al., 2019) and all decisions were made based on experience and instinct. Even though precision agriculture or precision farming began in the 1980s (Mulla, 2013), geospatial technology was used extensively in the early 2000 which involve the use of Geographic Information System (GIS), Remote Sensing (RS) and Unmanned Aerial Vehicles (UAV). Unlike the conventional method, these methods are able to track plant health effectively (Che Omar et al., 2019; Mulla, 2013; Sangeetha et al., 2019).

Unmanned Aerial Vehicles popularly known as UAV, is the latest technology for capturing all features of an object without touching the object. UAV has the ability to observe all objects in the horizontal and vertical direction (Ab Rahman et al., 2017; Abdul Maulud et al., 2019). Hassan et al. (2018) used UAVs in their study to determine the effectiveness of predicting wheat cultivation by using a multispectral approach in North China. This UAV platform can be used efficiently for field -based selection and grain yield prediction. While, Ivushkin et al. (2019) and Shi et al. (2016) used UAV to determine the salinity content and arsenic level of agriculture soil, respectively. These researchers found that the Photochemical reflection index (PRI) was able to estimate the soil conditions, especially salt stress and arsenic soils. This technology has also been used to detect problems related to irrigation systems in an olive grove in Barcelona, Spain (Jorge et al., 2019).

With the advancements in spatial technologies, a number of studies have been conducted in the rice sector by using GIS. The rice chlorophyll content can be assessed using five vegetation Indices (VIS) from the hyperspectral data, namely Normalized Difference Vegetation Index (NDVI), Modified Simple Ratio Index (MSR), Modified Chlorophyll Absorption Ratio Index (MCARI), Transformed Chlorophyll Absorption Ratio Index (TCARI), and Optimized Soil-Adjusted Vegetation Index (OSAVI) (Xu et al., 2011). Huang et al. (2013) attempted to estimate rice yield by using several NDVI variables, while Mosleh et al. (2015) explored the use of microwave RS to predict rice yield. These researchers found that NDVI always has a positive effect on paddy yield.

In 2018, Deng et al. discovered that VIs (NDVI and red-edge NDVI (reNDVI)) are not entirely dependent on reflectance accuracy. VI is widely used as an essential element in the monitoring and managing of many activities in agriculture, particularly regarding plant conditions (Hassan et al., 2018). Most of the indices have similar functions and use the inverse relationship between red with 630–690 nm wavelength and near-infrared (NIR) with 760–900 nm wavelength reflectance correlated with healthy green vegetation (Gao, 1996; Hunt et al., 2012; Liu et al., 2019; Lu and Zhuang, 2010; Migliavacca et al., 2018; Yebra et al., 2013) such as Normalized Difference Vegetation Index (NDVI) (Rouse et al., 1973), Blue Normalized Difference Vegetation Index (BNDVI) (Wang et al., 2007), and Normalized Difference Red Edge (NDRE) (Buschmann and Nagel, 1993).

NDVI is frequently used for monitoring vegetation cover and crop stress by using red band with 630–690 nm wavelength (Hunt et al., 2012). This VI is used to measure biomass in precision farming, and in forestry applications it is used to quantify forest supply and leaf area index (Huete et al., 2002; Junior et al., 2016). However, NDVI has its limitations, especially when used on dense crop, and may give inaccurate estimates of index values as a result of atmospheric contaminants (Xie et al., 2018; Yeom et al., 2019). According to Wang et al. (2007), BNDVI is an index which requires analysis of visible blue with 450–520 nm wavelength (Hunt et al., 2012) of the UAV aerial images. According to Avtar and Watanabe (2020), this index can be used to locate possible over-fertilized areas. Excessive use of fertilizers can affect the water quality of an area and this in consequent affect plant, animal and human health.

Conversely, NDRE is sensitive to the chlorophyll content of leaves against soil background effects. This index can only be formulated when the red edge band is available with 700–730 nm wavelength (Hunt et al., 2012). In addition, it is susceptible to changes in plants growth and has been proven to be more beneficial than NDVI (Jorge et al., 2019; Maccioni et al., 2001).

Despite the success of the VIs approach in agriculture, there is still inadequate information regarding the best vegetation index for dense crops, especially paddy plants, when measuring the level of plant growth. Previous research has predominantly focused on the growth stages of paddy plants at a single level, primarily utilizing typical vegetation indices such as NDVI and BNDVI. Consequently, the main goal of this research is to assess the performance of three vegetation indices (VIs), namely NDVI, BNDVI, and NDRE, in accurately depicting the health of paddy plants across three different stages of growth.

## 2. Methods and materials

This study was conducted in Kampung Padang Garam, Kuala Kedah, Malaysia which is on the west coast of Peninsular Malaysia as shown in Fig. 1. The study involved an area of approximately 20 ha of paddy field. This research involved two different paddy cultivation seasons for the period from May 2019 to January 2020. The first season was from May to September 2019, while the second season was from October 2019 to January 2020. The two seasons are classified as South-West Monsoon and North-East Monsoon by the Malaysia Meteorology Department (2019b). The weather during the South-West Monsoon can be extremely dry, while the North-East Monsoon is a wet season with heavy rainfall. The average temperature recorded during the investigation period is 32.7 and 33.3 degrees Celsius for season 1 and 2, respectively.

The study consists of two phases, UAV image acquisition and secondary data analysis, as illustrated in Fig. 2. The two phases are essential for obtaining the best data and facilitating the achievement of the objectives of the study.

The first phase of this study has been started by involving a UAV platform to capture multispectral images throughout the cultivation season from May 2019 until January 2020, as listed in Table 1.

Three flights were made throughout the season to in an effort to predict paddy growth condition on 40, 60, and 100 Day After Sowing (DAS), which represents the tillering, flowering and maturing stage, respectively, as illustrated in Fig. 3.

The UAV platform was prepared and equipped with the Micasense RedEdge-M multispectral camera sensor shown in Fig. 4. This camera sensor is an advanced multispectral camera specially designed for small unmanned aircraft systems. It provides accurate multiband data (red, green, blue, red-edge, and near-infrared) for agriculture remote sensing. In order to capture consistent multispectral images over time, the DroneDeploy mobile application was used to produce the flight plan and was connected to the DJI Inspire 2. According to Abdul Maulud et al. (2019); Arif et al. (2018); Zhang and Kovacs (2012), despite its low operational cost, the UAV platform is well-known to have high spatial and temporal resolution and is easy to handle during the image acquisition stage.

Thousands of aerial images were captured during acquisition and subsequently processed and analyzed using the Agisoft Metashape and ArcGIS software, which uses a spatial analysis approach. The Agisoft Metashape software encompasses a series of seven distinct stages for multispectral processing. These stages involve essential post-imagery processing procedures, which include: (1) the importing of multispectral images; (2) the computing of camera reflectance; (3) the aligning and optimizing of the camera; (4) the reconstructing of the surface; (5) the generating of an orthomosaic; (6) the calculating of indices utilizing raster calculator tools; and (7) the exporting of the resulting data.

Three vegetation indices were selected for examination in this study, namely, NDVI, NDRE and BNDVI. These VIs were calculated using raster transform in the sixth processing stage using the following formulas:
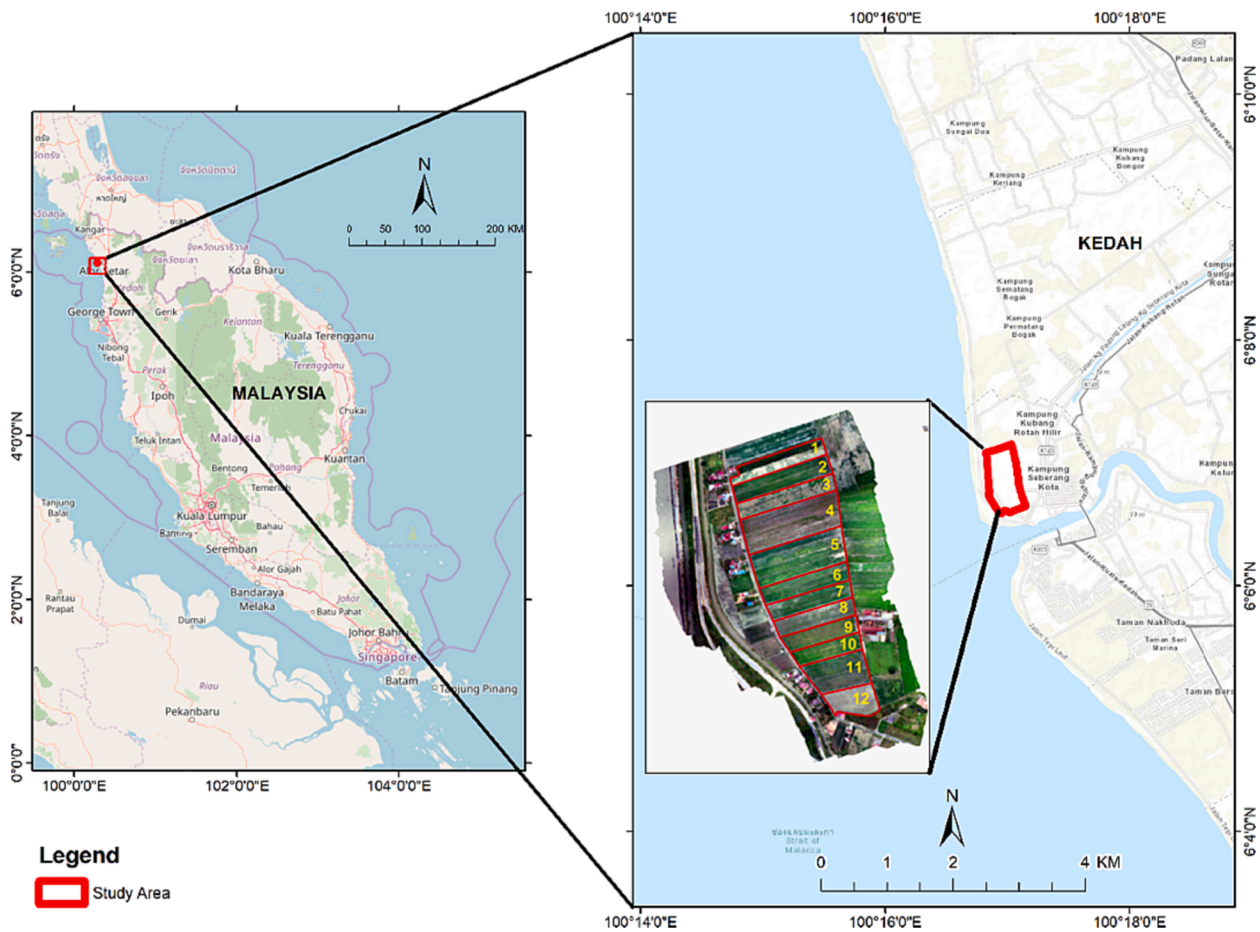
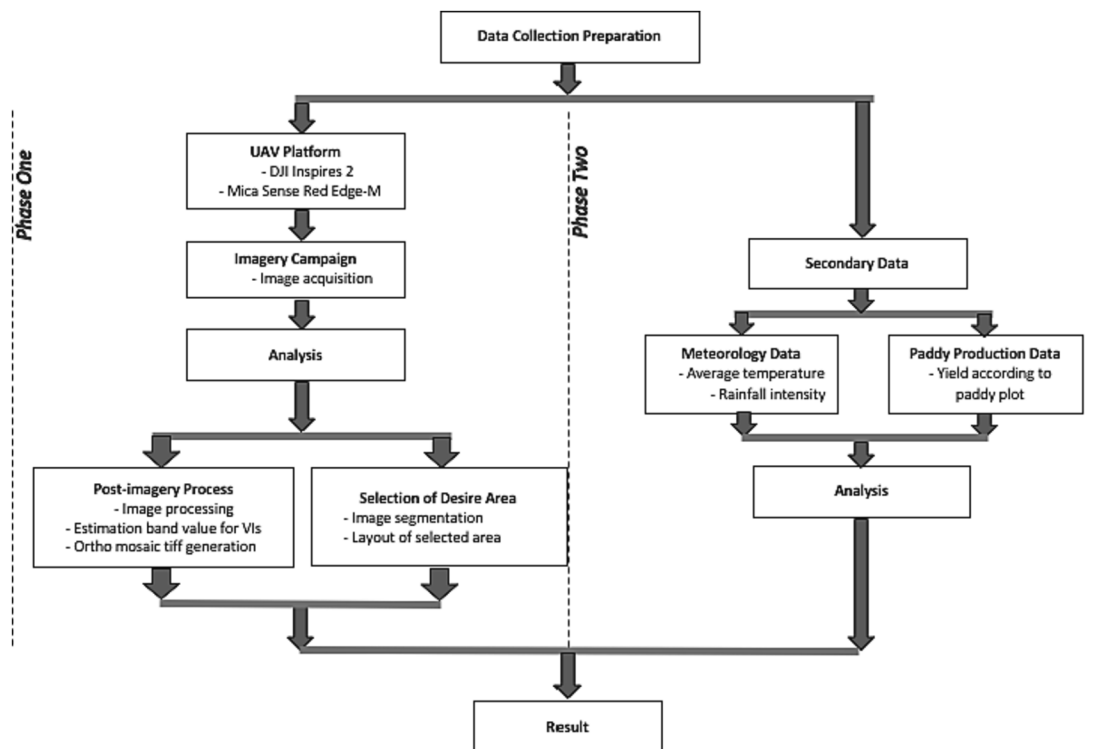**Fig. 1.** Study area comprising 12 paddy plots in Kuala Kedah, Malaysia.



**Fig. 2.** Phases in the methodology.

**Table 1**
UAV acquisition during season 1–2019 and season 2–2019.

| Growth Stage | Season 1–2019 | Season 2–2019 |
|---|---|---|
| 40 DAS | 28 Jun 2019 | 20 Nov 2019 |
| 60 DAS | 18 Jul 2019 | 7 Dec 2019 |
| 100 DAS | 27 Aug 2019 | 15 Jan 2020 |

Note: DAS = Day After Sowing.

$$NDVI = \frac{(NIR - Red)}{(NIR + Red)} \quad \text{(Rouse et al., 1973)} \tag{1}$$

$$BNDVI = \frac{(NIR - Blue)}{(NIR + Blue)} \quad \text{(Wang et al., 2007)} \tag{2}$$

$$NDRE = \frac{(NIR - RedEdge)}{(NIR + RedEdge)} \quad \text{(Buschmann \& Nagel, 1993)} \tag{3}$$

The orthomosaic images with different VIs values were identified by converting the raster image into a vector. The index value was generated through several processes in ArcGIS: (1) raster clipping to cut the raster image according to the paddy plot area; (2) raster reclassify to classify the index values, as shown in Table 2; (3) converting tools to transform the raster into a polygon; and (4) calculate the area for each VI based on the index value categories, as shown in Table 2.

Subsequently, the implementation of phase two entailed the collection of required secondary data from relevant local agencies. The meteorological data, encompassing average temperature and rainfall intensity statistics, were collected from the Department of Meteorology Malaysia. The paddy production data was obtained from the local government as well as the main national regulatory authorities involved in the production chain, namely MADA and Beras Nasional (BERNAS). The rice production data for Seasons 1–2019 and 2–2019 were collected and organized according to plot number and farmer's name.

## 3. Results and discussion

### 3.1. Correlation between index value, yield and plot area

Fig. 5 shows the amount of rice produced in Season 1 and Season 2, as recorded by BERNAS. The figure shows that three plots (plot-1, plot-7 and plot-12) do not have a value as the farmers did not declare their yield to BERNAS. According to the statistics provided by BERNAS for Season 1 and Season 2, each plot showed a positive increasing trend in rice production. Three plots recorded the highest increase of 25%, namely plot-2, plot-3 and plot-9, while the yield for plot-5, plot-10 and plot-11 showed an increase of less than 10%. However, plot-8 recorded a reduction of about 0.2%.

Based on the observation, despite having a large paddy cultivation area, it does not promise more yield than a small area, as revealed in Fig. 5. This figure clearly shows the higher yield was recorded from plot-9 and plot-10, which have smaller plot areas compared to plot-4 and plot-5. This is indicates that the yield is directly or indirectly influenced by a number of factors, especially environmental factors and proper

agricultural practices, which aligned with a report by (Ceyhan et al., 2012; Singh and Singh, 2016).

Therefore, the plant's conditions were examined on the basis of the NDVI, BNDVI and NDRE values. During Season 1, the average production for the 12 plots is 2,842 kg per hectare compared to the 3,428 kg per hectare recorded for Season 2. Fig. 6 shows the higher VI values for both



**Fig. 4.** DJI Inspire 2 equipped with MicaSense RedEdge-M camera sensor.

**Table 2**
Category based on the values of VIs (Akmal et al., 2011; Giacomo & David, 2018; Hashim et al., 2019; Jesslyn, 2015; Zaitunah et al., 2018).

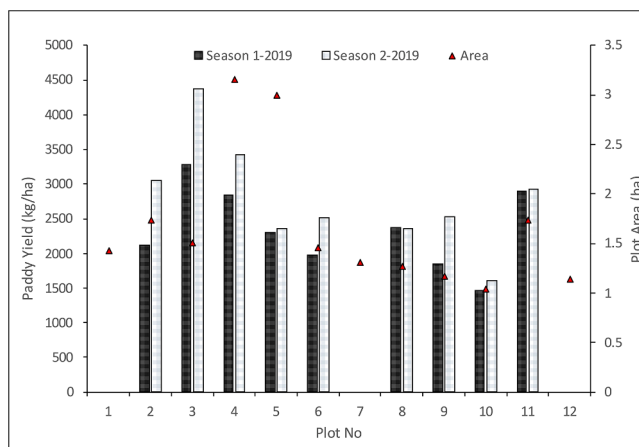| Index Value | Description |
|---|---|
| < 0 | No vegetation or plant |
| 0 to 0.1 | Poor vegetation density |
| 0.1 to 0.3 | Moderate vegetation density |
| 0.3 to 0.6 | High vegetation density |
| 0.6 to 1.0 | Very-high vegetation density |



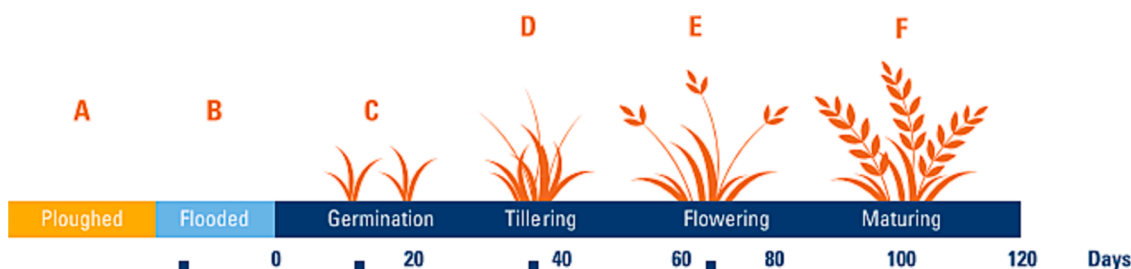**Fig. 5.** Plot area and rice production for Season 1–2019 and Season 2– 2019.



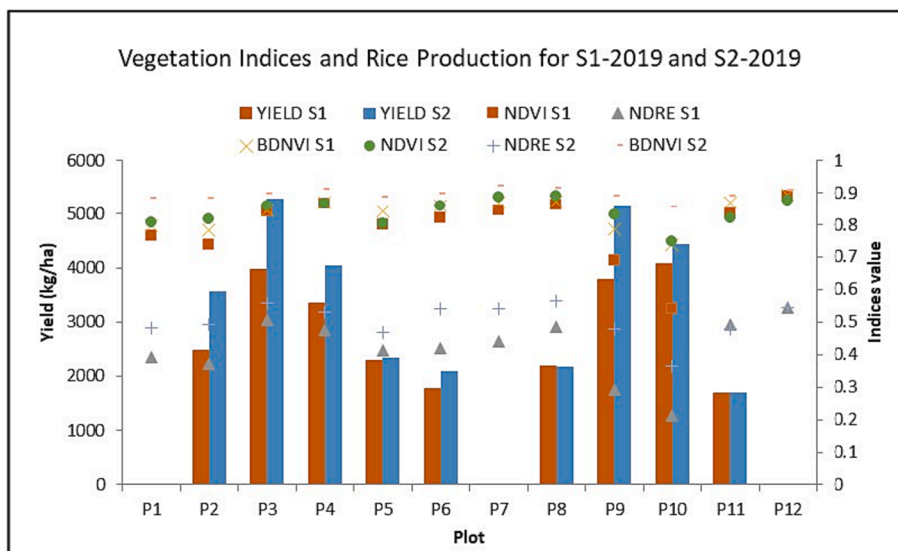**Fig. 3.** Stages of paddy growth (Che Omar et al., 2019).

**Fig. 6.** Index values versus rice production for Season 1–2019 and Season 2– 2019.

seasons.

NDRE appears to have the lowest value, with an average value of 0.409 and 0.504 for season 1 and 2, respectively, which is categorized as High Density Vegetation. Meanwhile, NDVI and BNDVI are in the Very High Density Vegetation class with average values of 0.782 and 0.839, and 0.831 and 0.895 for season 1 and 2, respectively. Therefore, in the context of the VIs approach used in plants monitoring, NDRE provides a more accurate value compared to NDVI and BNDVI. This scenario and

findings are congruent with the findings reported by Jorge et al. (2019) and Lu and Zhuang (2010). Additionally, the trend for both VI and rice production indicates a strong relationship between the two parameters compared to yield, as discussed in the previous paragraph. There is a 21 percent increase in rice production, and the increase of 23 percent in NDRE is significantly higher that the increase of 8 percent recorded for both NDVI and BNDVI.

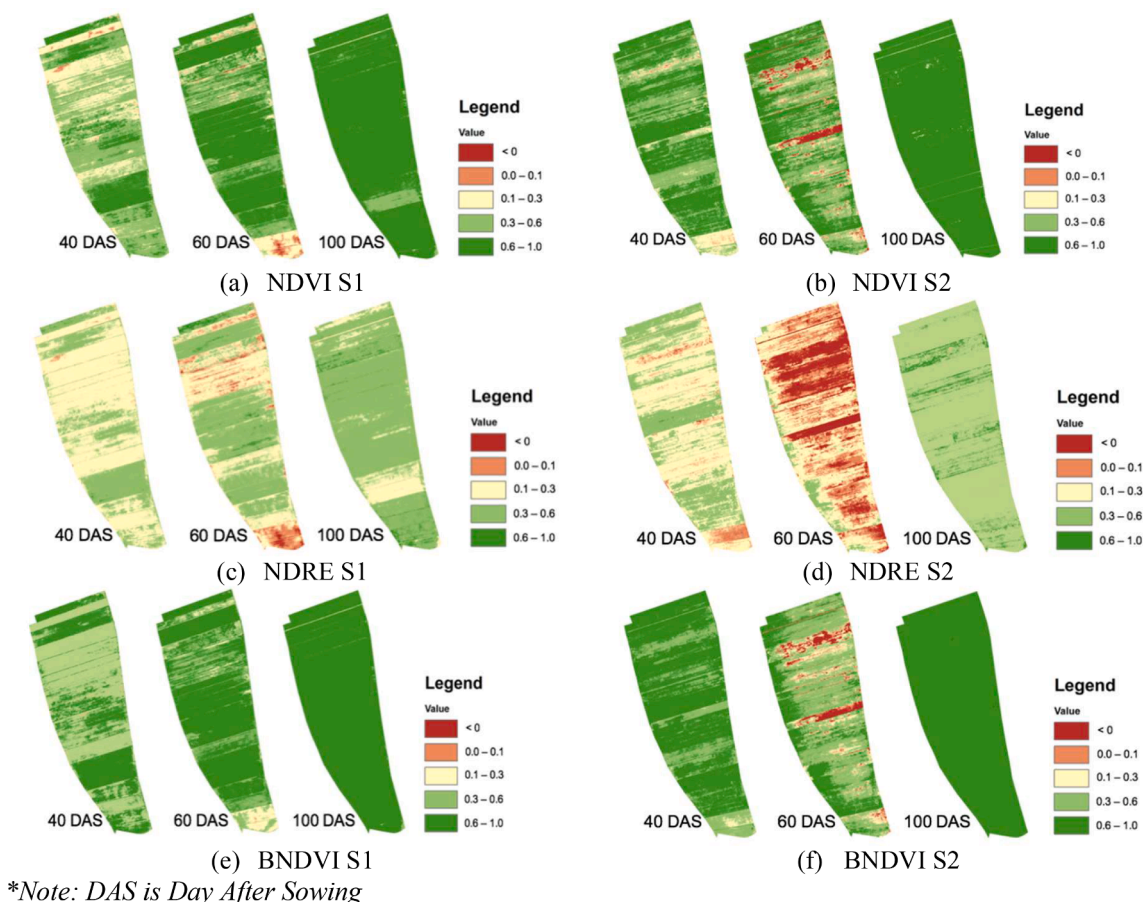In addition, this VIs assessment is also made based on the paddy



(a)  NDVI S1



(b)  NDVI S2



(c)  NDRE S1



(d)  NDRE S2



(e)  BNDVI S1



(f)  BNDVI S2

*Note: DAS is Day After Sowing*

**Fig. 7.** Map of vegetation index for Season 1–2019 and Season 2–2019. *Note: DAS is Day After Sowing.*

growth stages for both seasons. Each VI is represented by five categories, as shown in Table 2. The values for Season 1–2019 show that the highest area percentage of NDVI and BNDVI changed from high vegetation density on 40 DAS to very high vegetative density on 60 DAS and 100 DAS. However, the NDRE showed a change from moderate vegetative density on 40 DAS to high vegetation density on 60 DAS. These results are congruent with those reported by Carneiro et al. (2019), where NDRE has a higher correlation with productivity values on 60 DAS. The percentage difference for NDVI and NDRE during this season is 65 percent, 53 percent and 92 percent for 40, 60 and 100 DAS, respectively.

Generally, the paddy plants grew at an acceptable range during Season 1–2019. In contrast, the growth during Season 2–2019 was relatively unstable due to environmental factors, namely the South-West and North-East Monsoon seasons. However, the results of field observations and analysis show that the NDRE values represent the best actual condition of the plants compared to the values of NDVI and BNDVI. This result is similar to those reported by Jorge et al. (2019) and Lu and Zhuang (2010) where the accuracy of NDRE is better than those for NDVI and BNDVI.

### 3.2. Mapping and evaluation of VI values for three different growth stage

The map in Fig. 7 shows the NDVI, BNDVI and NDRE values for the three growth stages during Season 1–2019 and Season 2–2019. These figures clearly show the actual scenario for each growth stage. The NDRE maps show a more accurate variation of the actual situation in the field for both seasons. However, the maps for NDVI and BNDVI show similarity in terms of color distribution.

Fig. 8 and Fig. 9 show the percentage of NDVI, BNDVI and NDRE during three different growth stages for both seasons. Each VI is represented by five categories, as shown in Table 2. The values for Season 1–2019 show that the highest area percentage of NDVI and BNDVI changed from high vegetation density on 40 DAS to very high vegetative density on 60 DAS and 100 DAS. However, the NDRE showed a change from moderate vegetative density on 40 DAS to high vegetation density on 60 DAS. These results are congruent with those reported by Carneiro et al. (2019), where NDRE has a higher correlation with productivity values on 60 DAS. The percentage difference for NDVI and NDRE during this season is 65 percent, 53 percent and 92 percent for 40, 60 and 100 DAS, respectively.

In addition, the trends for NDVI and BNDVI during Season 2–2019 are similar to those during Season 1–2019 with the exception of the pattern for NDRE. During Season 2–2019, the change in the highest area of NDRE recorded a moderate vegetation density on 40 DAS and 60 DAS to high vegetation density on 100 DAS. The percentage difference for NDVI and NDRE during this season is 83 percent, 7 percent and 99 percent for 40, 60 and 100 DAS, respectively.

Generally, the paddy plants grew at an acceptable range during Season 1–2019. In contrast, the growth during Season 2–2019 was relatively unstable due to environmental factors, namely the South-West and North-East Monsoon seasons. However, the results of field observations and analysis show that the NDRE values represent the best actual condition of the plants compared to the values of NDVI and BNDVI. This result is similar to those reported by Jorge et al. (2019) and Lu and Zhuang (2010) where the accuracy of NDRE is better than those for NDVI and BNDVI.

### 3.3. Mapping and evaluation of VI values for three different growth stages by plot

For a detailed analysis, the map was analyzed on the basis of the condition of each paddy plot, as shown in Fig. 10. Twelve plots were identified and analyzed in this study based on the ownership of the plot.

Fig. 11a shows the percentage of NDVI for the area at 40, 60 and 100 DAS based on the plot number. With the exception of plot 12, all plots showed a good growth increment throughout the growth stage.

The NDVI values showed a good plant density in the first stage of growth (40 DAS), and the values decreased slightly in the second stage of growth (60 DAS). In contrast, the plants' condition was recorded in a moderate vegetation density category. However, the value increased to very-high vegetation density during the third stage of growth (100 DAS). This trend is similar to the pattern observed for the BNDVI value in Fig. 11b.

In addition, as can be seen in Fig. 11c, the trend for NDRE values was similar to that of NDVI values, where the value was significant in the first stage of growth but decreased during the second stage, and returned to a good condition in the third stage of growth. Surprisingly, 10 of the 12 plots showed a lower value during the second stage. The two plots that showed an increase are plots 9 and 10.

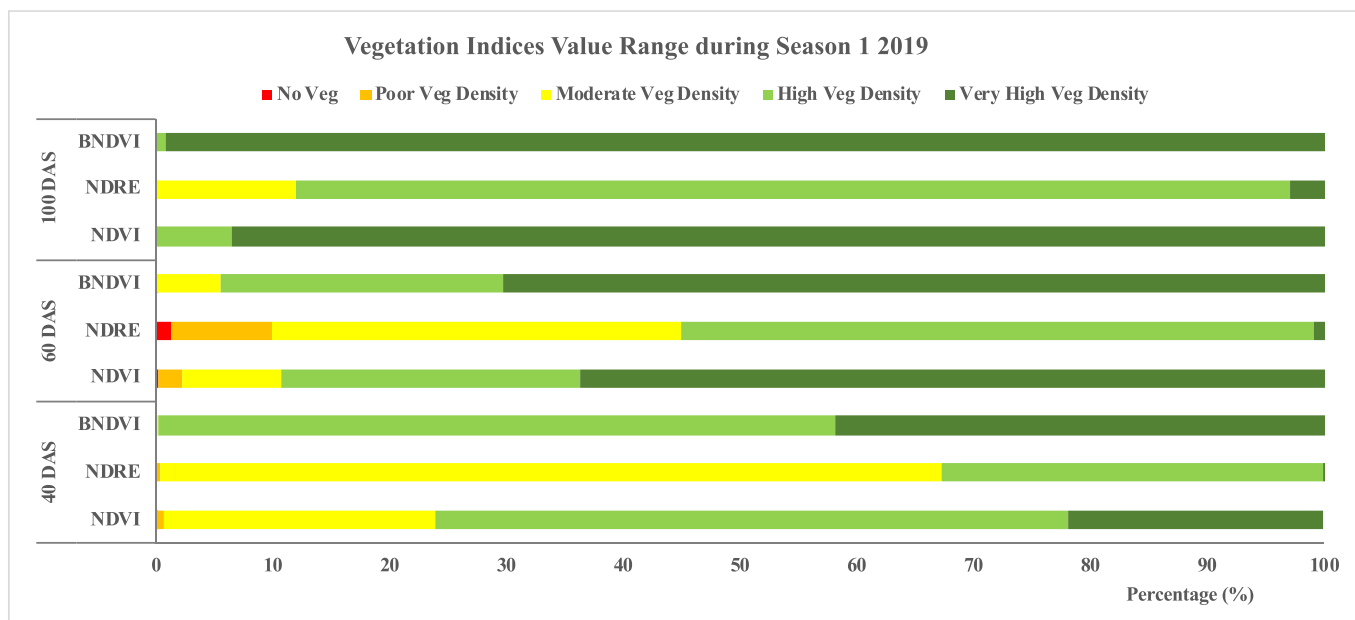The results for Season 2–2019 showed that the value for each index is



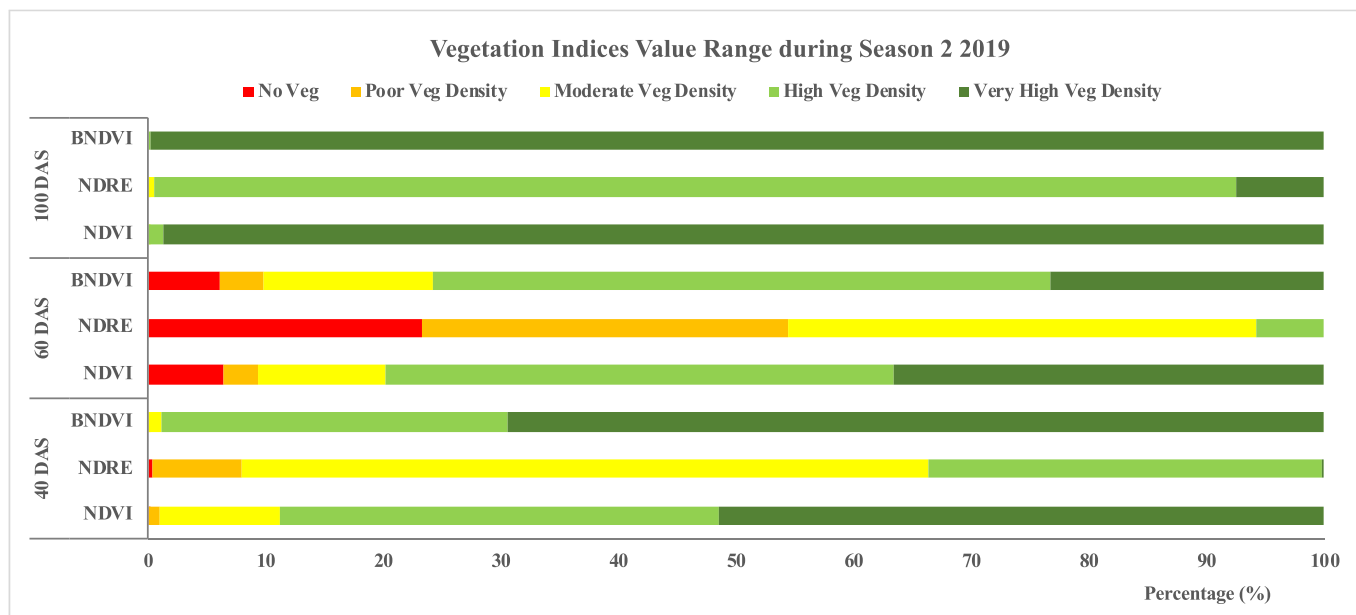**Fig. 8.** Range of vegetation index during Season 1–2019.

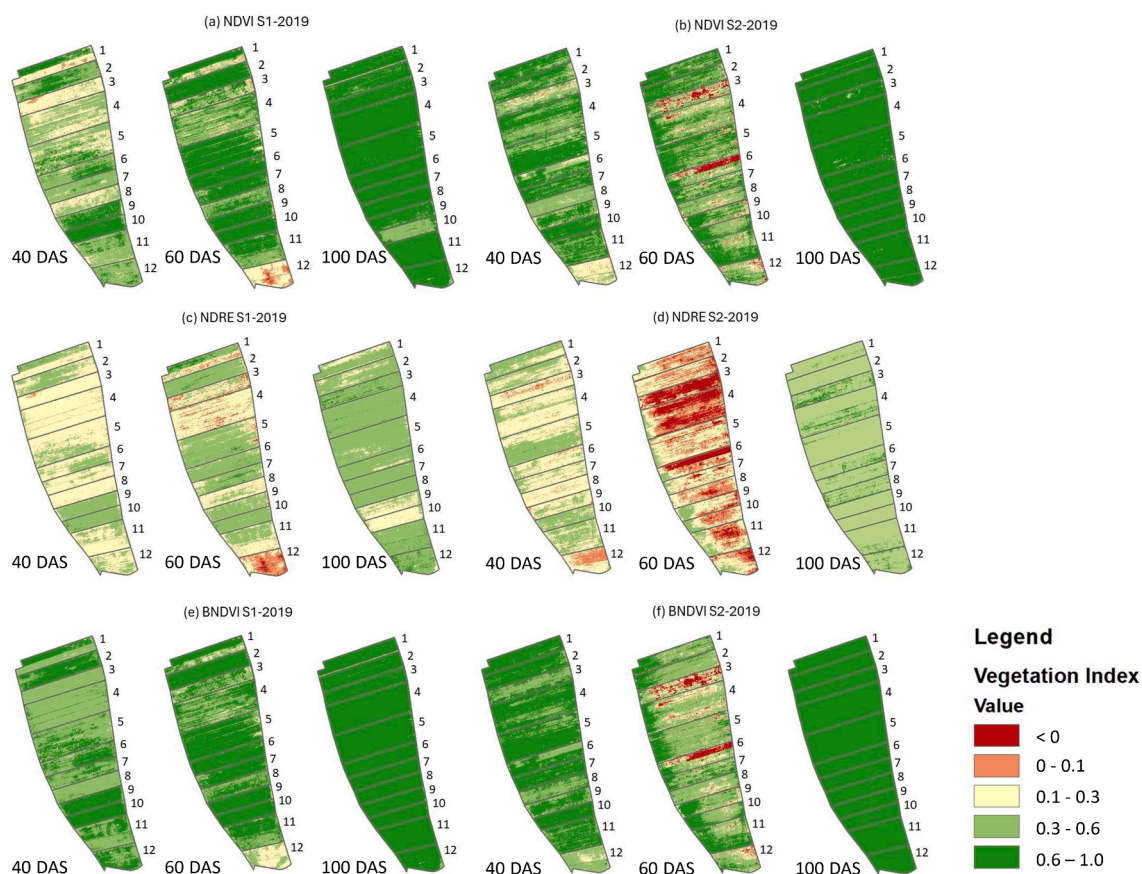**Fig. 9.** Range of vegetation index during Season 2–2019.



**Fig. 10.** Map of vegetation index for each plot during Season 1–2019 and Season 2–2019.

similar, as can be seen in Fig. 12a, Fig. 12b and Fig. 12c. Each index showed a fluctuation in the value of paddy plots for the entire season. The trends for NDVI, BNDVI and NDRE values are comparable with those for Season 1–2019. The vegetation density, however, showed a deterioration in the second phase and the value is considerably higher than the value from the previous season.

Fig. 12b shows that there is a problem with regard to the fertilizer used and 9 of the 12 plots were adversely affected in the flowering stage. The red color in the figure indicates that less fertilizer was used compared to that with green color, and this has had an impact on plant growth; this scenario can be classified as current fertilizer levels in the plots (Avtar and Watanabe, 2020). As reported by the Malaysian
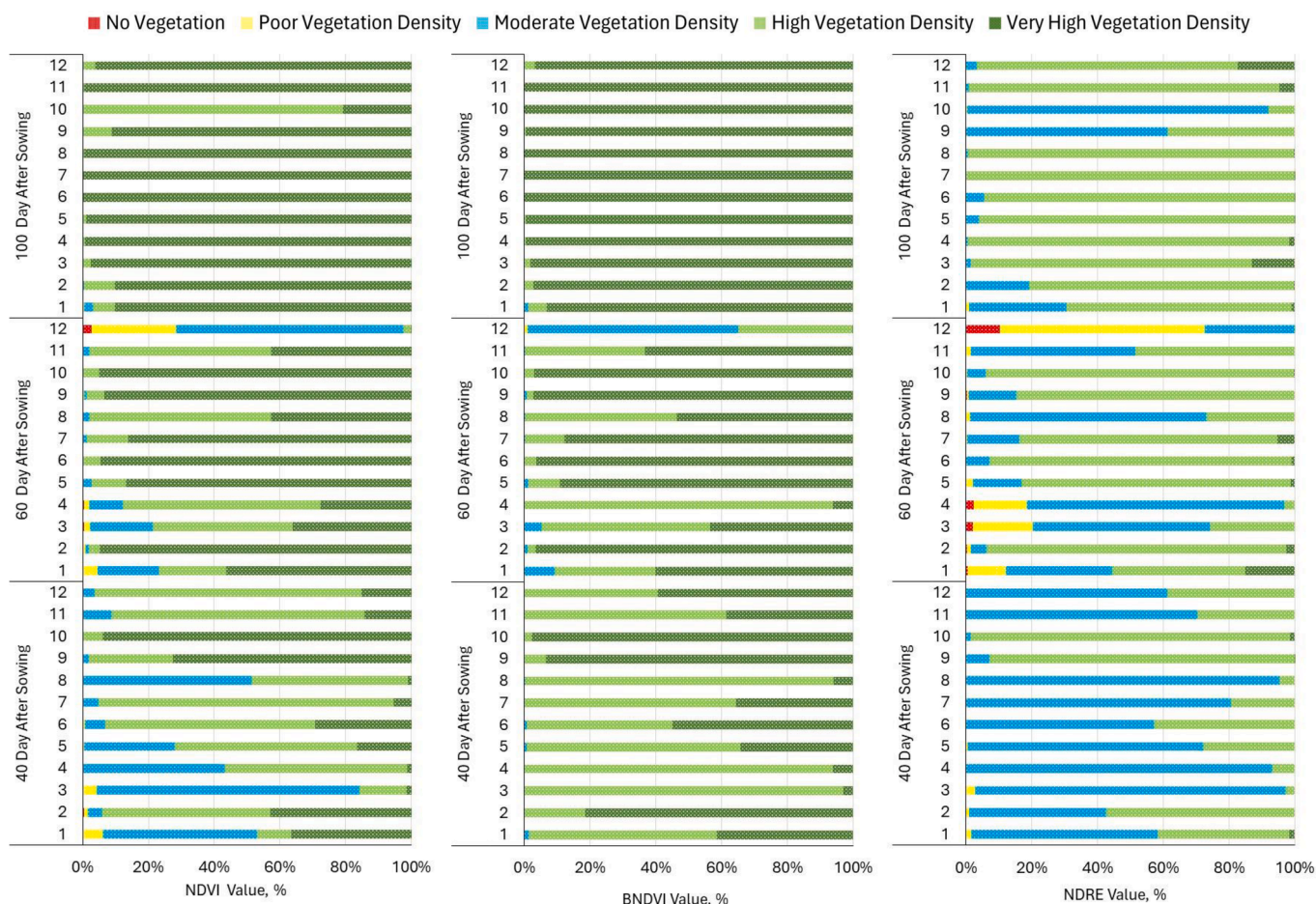
**Fig. 11.** Different VIs values according to plot number during Season 1–2019 using. (a) NDVI; (b) BNDVI; and (c) NDRE.

Meteorological Department (2019a), the lack of rainfall in Kedah has resulted in reduced water levels in the paddy plot. The soil became extremely dry, and this has adversely affected the paddy plants, where there was a deterioration in the plant's growth and the plants were even destroyed due to the inadequate amount of fertilizer used (Osakabe et al., 2014; Rad et al., 2012; Salehi Lisar et al., 2012). Additionally, contaminated irrigation water also affects the soil fertility, which has an adverse effect on plant growth (Aboelsoud et al., 2022; El Baroudy et al., 2020).

Generally, both seasons showed a decreasing trend for the VI values on 40 DAS, which then increased to 100 DAS. During the period of up to 60 DAS, the rice plots were in a watery state and the paddy plants were able to grow well into dense crops despite the turbulent flow (Sharil et al., 2016) caused by factors such as heavy rains and strong winds. The amount of water in the rice plots was reduced upon entering the 100 DAS stage to ensure that the rice seeds reach maturity and could be harvested at the right time. However, the VI values showed a positive increase, which indicates better condition of the plants.

Overall, the results show the index value for each VI increased during Season 1–2019 and Season 2–2019. Among these three VIs, NDRE shows a lower value than the other VI because it is more sensitive to changes in chlorophyll content that affect the color of plant leaves. As reported by Abdelrahman et al. (2022), plants exhibiting less photosynthetic capacity tend to exhibit heightened reflectance in the visible spectrum - while displaying reduced reflectance in the near-infrared (NIR) range. However, through statistical analysis, NDRE gives a more accurate value with R square values of 0.842 compared to 0.706 and 0.575, respectively, for NDVI and BNDVI values, even though these three VI have p values <0.05.

## 4. Conclusion

The demand for rice in Malaysia increases each year despite the scarce resources needed to produce rice, especially land. As a major contributor to the economic sector, rice cultivation activities have to be monitored and managed appropriately. Even though the harvested plot area is bigger, there is no assurance of higher yield compared to the smaller harvested plot area. Therefore, geospatial technology approaches have been used to monitor field conditions on a regular basis to ensure that the targeted maximum yield is achieved to meet national demand. The high accuracy UAV fitted with excellent resolution Red-Edge Multispectral camera was able to produce good results in the effort to establish a monitoring framework for better rice management. The percentage difference for NDVI and NDRE during Season 2–2019 is higher than that for Season 1–2019. Based on a comparison of the NDVI and NDRE values, it can be concluded that NDRE gives a more significant, accurate, and reliable value. The value for BNDVI is a reliable index that represents the actual condition of plants, especially during the fertilization activity in the cultivation cycle. In conclusion, VIs is instrumental in the monitoring of crop growth in the field, which is beneficial for all stakeholders, like farmers, local authorities, and the government. The utilization of remote sensing technology holds significant importance in the evaluation of the influence of climate change on rice cultivation. The integration of temperature, precipitation, soil moisture, and vegetation indicators into monitoring systems can contribute to the development of agricultural methods that are robust to climate change.
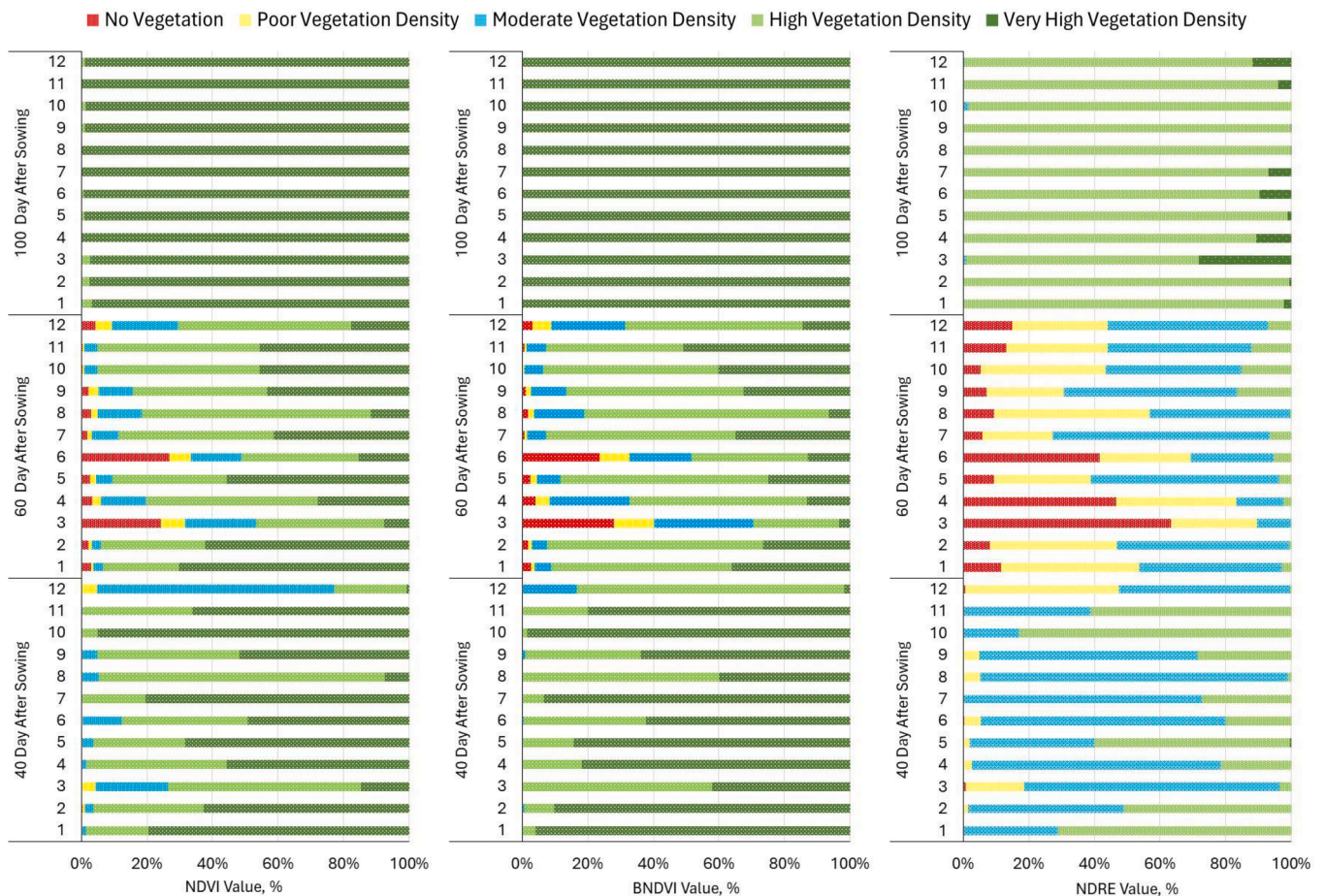
**Fig. 12.** Different VI values according to plot number during Season 2–2019: (a) NDVI; (b) BNDVI; (c) NDRE.

## Declaration of Competing Interest

The authors declare that they have no known competing financial interests or personal relationships that could have appeared to influence the work reported in this paper.

## Acknowledgements

## References

Ab Rahman, A.A., Abdul Maulud, K.N., Mohd, F.A., Jaafar, O., Tahar, K.N., 2017. Volumetric calculation using low cost unmanned aerial vehicle (UAV) approach. IOP Conf. Series: Mater. Sci. Eng. 270 (1) https://doi.org/10.1088/1757-899X/270/1/012032.

Abdelrahman, M.A.E., Afifi, A.A., D'antonio, P., Gabr, S.S., Scopa, A., 2022. Detecting and mapping salt-affected soil with arid integrated indices in feature space using multi-temporal landsat imagery. Remote Sens. (Basel) 14 (11). https://doi.org/10.3390/rs14112599.

Abdelrahman, A.E. M., Engel, S.M., Eid, M., & Aboelsoud, H.M. 2022. A new index to assess soil sustainability based on temporal changes of soil measurements using geomatics–an example from El-Sharkia, Egypt. *All Earth* 34(1) 147–166. doi: 10.1080/27669645.2022.2103953.

Abdul Hamid, Z. 2018, December 31. *Climate change and human health.* https://www.nst.com.my/opinion/columnists/2018/12/445565/climate-change-and-human-health.

Abdul Maulud, K.N., Arif, F., Ab Rahman, A.A. 2019. Low-cost UAV for determination of horizontal and vertical coordinates changes near coastal area. In: *40th Asian*

Conference on Remote Sensing, ACRS 2019: Progress of Remote Sensing Technology for Smart Future, 3(October), 1979–1984.

Aboelsoud, H.M., AbdelRahman, M.A.E., Kheir, A.M.S., Eid, M.S.M., Ammar, K.A., Khalifa, T.H., Scopa, A., 2022. Quantitative estimation of saline-soil amelioration using remote-sensing indices in arid land for better management. Land 11 (7), 1–19. https://doi.org/10.3390/land11071041.

Akmal, S., Syarina, M.S., Mastura, S.A.S., Ghaffar, M.A., 2011. Towards the conservation of Sungai Santi catchment: monitoring of land use and vegetation density of mangrove areas. J. Trop. Mar. Ecosyst. 1 (1), 9–21.

Amedie, F.A. 2013. Impacts of Climate Change on Plant Growth, Ecosystem Services, Biodiversity , and Potential Adaptation Measure. 1–61.

Arif, F., Ab Rahman, A.A., Abdul Maulud, K.N., 2018. Low-cost unmanned aerial vehicle photogrammetric survey and its application for high-resolution shoreline changes survey. In: Proceedings Asian Conference on Remote Sensing, pp. 1391–1395.

Avtar, R., Watanabe, T. (Eds.). 2020. *Unmanned Aerial Vehicle Applications in Agriculture and Environment* (1st ed.). Springer Nature Switzerland AG. doi: 10.1007/978-3-030-27157-2.

Buschmann, C., Nagel, E., 1993. In vivo spectroscopy and internal optics of leaves as basis for remote sensing of vegetation. Int. J. Remote Sens. 14 (4), 711–722. https://doi.org/10.1080/01431169308904370.

Carneiro, F.M., Furlani, C.E.A., Zerbato, C., Menezes, P.C. De, & Gírio, L.A.S. 2019. Correlations among vegetation indices and peanut traits during different crop development stages. *Engenharia Agrícola, 4430*(Special Issue: Precision Agriculture), 33–40. doi: https://doi.org/10.1590/1809-4430-Eng.Agric.v39nep33-40/2019 Special.

Ceyhan, E., Kahraman, A., Onder, M., 2012. The impacts of environment on plant products. Int. J. Biosci. Biochem. Bioinf. 2 (1), 48–51. https://doi.org/10.7763/ijbbb.2012.v2.68.

Che Omar, S., Shaharudin, A., Tumin, S. A. 2019. The status of the paddy and rice industry in Malaysia. In: *The Status of the Paddy and Rice Industry in Malaysia.*

Deng, L., Mao, Z., Li, X., Hu, Z., Duan, F., Yan, Y., 2018. UAV-based multispectral remote sensing for precision agriculture : A comparison between different cameras. ISPRS J. Photogramm. Remote Sens. 146 (March), 124–136. https://doi.org/10.1016/j.isprsjprs.2018.09.008.

El Baroudy, A.A., Ali, A.M., Mohamed, E.S., Moghanm, F.S., Shokr, M.S., Savin, I., Poddubsky, A., Ding, Z., Kheir, A.M.S., Aldosari, A.A., Elfadaly, A., Dokukin, P., Lasaporara, R., 2020. Modeling land suitability for rice crop using remote sensing and soil quality indicators: The case study of the Nile delta. Sustainability (Switzerland) 12 (22), 1–25. https://doi.org/10.3390/su12229653.

FAO. 2019. *Crops and livestock products*. Food and Agriculture Organisation of the United Nations. http://www.fao.org/faostat.

Fikri Abdullah, A., Wan Mustapa, W.A., 2016. Groundwater conceptual model for paddy irrigation. Jurnal Teknologi 78 (1–2), 111–117. https://doi.org/10.11113/jt.v78.7283.

Gain, P., Mannan, M.A., Pal, P.S., Hossain, M.M., Parvin, S., 2004. Effect of Salinity on Some Yield Attributes of Rice. Pak. J. Biol. Sci. 7, 760–762. https://doi.org/10.3923/pjbs.2004.760.762.

Gao, B.-C., 1996. NDWI - A normalized difference water index for remote sensing of vegetation liquid water from space. Remote Sens. Environ 58, 257–266.

Giacomo, R., David, G. 2018. E-Agriculture in action: Drones for agriculture. In: G. Sylvester (Ed.), *Food and Agriculture Organization of the United Nations and International Telecommunication Union* (pp. 9–25). FAO and ITU. http://www.fao.org/3/i8494en/i8494en.pdf.

Hashim, H., Abd Latif, Z., Adnan, N.A. 2019. Urban vegetation classification with Ndvi threshold value method with very high resolution (Vhr) Pleiades imagery. In: *6th International Conference on Geomatics and Geospatial Technology*, XLII-4/W16, 237–240. doi: 10.5194/isprs-archives-xlii-4-w16-237-2019.

Hassan, M.A., Yang, M., Rasheed, A., Yang, G., Reynolds, M., Xia, X., Xiao, Y., He, Z. 2018. A rapid monitoring of NDVI across the wheat growth cycle for grain yield prediction using a multi-spectral UAV platform. *Plant Sci.*, *2018*, 1–9. doi: 10.1016/j.plantsci.2018.10.022.

Herman, T., Murchie, E.H., Warsi, A.A., 2015. Rice production and climate change: A case study of Malaysian rice. Pertanika J. Trop. Agric. Sci. 38 (3), 321–328.

Huang, J., Wang, X., Li, X., Tian, H., Pan, Z. (2013). *Remotely Sensed rice yield prediction using multi-temporal NDVI data derived from NOAA's-AVHRR*. 8(8), 1–13. doi: 10.1371/journal.pone.0070816.

Huete, A., Didan, K., Rodriguez, E.P., Gao, X., Ferreira, L.G., 2002. Overview of the radiometric and biophysical performance of the MODIS vegetation indices. Remote Sens. Environ. 83, 195–213. https://doi.org/10.1016/S0034-4257(02)00096-2.

Hunt, E.R., Doraiswamy, P.C., McMurtrey, J.E., Daughtry, C.S.T., Perry, E.M., Akhmedov, B., 2012. A visible band index for remote sensing leaf chlorophyll content at the Canopy scale. Int. J. Appl. Earth Obs. Geoinf. 21 (1), 103–112. https://doi.org/10.1016/j.jag.2012.07.020.

Ivushkin, K., Bartholomeus, H., Bregt, A.K., Pulatov, A., Franceschini, M.H.D., Kramer, H., Van Loo, E.N., Jaramillo, V., Finkers, R., 2019. UAV based soil salinity assessment of cropland. Geoderma 338 (May 2018), 502–512. https://doi.org/10.1016/j.geoderma.2018.09.046.

Jesslyn, B., 2015. NDVI, the Foundation for Remote Sensing Phenology. U.S. Geological Survey (USGS) https://www.usgs.gov/land-resources/eros/phenology/science/ndvi-foundation-remote-sensing-phenology?qt-science_center_objects=0#qt-science_center_objects.

Jorge, J., Vallbé, M., Soler, J.A., 2019. Detection of irrigation inhomogeneities in an olive grove using the NDRE vegetation index obtained from UAV images. Eur. J. Rem. Sens. 52 (1), 169–177. https://doi.org/10.1080/22797254.2019.1572459.

Junior, C. K., Guimarães, A. M., Caires, E. F. (2016). Use of active canopy sensors to discriminate wheat response to nitrogen fertilization under no-tillage. *Engenharia Agríc.*, *36*(5), 886–886. doi: 10.1590/1809-4430-ENG.AGRIC.V36N5P886-894/2016.

Liu, B., Liu, H., Cao, W., Tian, Y., Cheng, T., Yao, X., Zhu, Y., Cao, Z., 2019. Comparison of the abilities of vegetation indices and photosynthetic parameters to detect heat stress in wheat. Agric. For. Meteorol. 265, 121–136. https://doi.org/10.1016/j.agrformet.2018.11.009.

Lu, X., Zhuang, Q., 2010. Evaluating evapotranspiration and water-use efficiency of terrestrial ecosystems in the conterminous United States using MODIS and AmeriFlux data. Remote Sens. Environ. 114 (9), 1924–1939. https://doi.org/10.1016/j.rse.2010.04.001.

Maccioni, A., Agati, G., Mazzinghi, P., 2001. New vegetation indices for remote measurement of chlorophylls based on leaf directional reflectance spectra. J. Photochem. Photobiol. B Biol. 61 (1–2), 52–61. https://doi.org/10.1016/S1011-1344(01)00145-2.

Mahmood, A., Latif, T., Arif Khan, M., 2009. Effect of salinity on growth, yield and yield components in basmati rice germplasm. Pak. J. Bot.

Malaysia Meteorology Department. (2019a). *Buletin Meteorologi Pertanian 10 Hari Dekad Ketiga Disember 2019* (Vol. 2019, Issue 2).

Malaysia Meteorology Department. (2019b). *Buletin Meteorologi Pertanian 10 Hari Dekad Pertama Disember 2019* (Vol. 2019).

Marfai, M.A., 2011. Impact of coastal inundation on ecology and agricultural land use case study in central Java, Indonesia. *Quaest. Geograph.* 30 (3), 19–32. https://doi.org/10.2478/v10117-011-0024-y.

Migliavacca, M., Simmer, C., van der Tol, C., Schneider, F.D., Morsdorf, F., Paul-Limoges, E., Damm, A., Rascher, U., Haghighi, E., 2018. Remote sensing of plant-water relations: An overview and future perspectives. J. Plant Physiol. 227, 3–19. https://doi.org/10.1016/j.jplph.2018.04.012.

Mosleh, M. K., Hassan, Q. K., & Chowdhury, E. H. (2015). *Application of Remote sensors in mapping rice area and forecasting its production: A review. i*, 769–791. doi: 10.3390/s150100769.

Mulla, D.J., 2013. Twenty five years of remote sensing in precision agriculture: Key advances and remaining knowledge gaps. Biosyst. Eng. 114 (4), 358–371. https://doi.org/10.1016/j.biosystemseng.2012.08.009.

Ngoc Thuy, N., Ha Anh, H. 2016. Vulnerability of rice production in Mekong River delta under impacts from floods, salinity and climate change. *Int. J. Adv. Sci. Eng. Inf. Technol.*. doi: 10.18517/ijaseit.5.4.545.

Osakabe, Y., Osakabe, K., Shinozaki, K., Tran, L.S.P., 2014. Response of plants to water stress. Front. Plant Sci. 5 (MAR), 1–8. https://doi.org/10.3389/fpls.2014.00086.

Rad, H.E., Aref, F., Rezaei, M., Amiri, E., Khaledian, M.R., 2011. The effects of salinity at different growth stage on rice yield. Ecol. Environ. Conserv.

Rad, H.E., Aref, F., Rezaei, M., 2012. Response of rice to different salinity levels during different growth stages. Res. J. Appl. Sci. Eng. Technol. 4 (17), 3040–3047.

Rouse, J.W., Hass, R.H., Schell, J.A., Deering, D.W. 1973. Monitoring vegetation systems in the Great Plains with ERTS. In: *Third Earth Resources Technology Satellite (ERTS) Symposium*, *1*, 309–317. doi: citeulike-article-id:12009708.

Sakaguchi, A., Eguchi, S., Kasuya, M., 2014. Examination of the water balance of irrigated paddy fields in SWAT 2009 using the curve number procedure and the pothole module. Soil Sci. Plant Nutr. 60 (4), 551–564. https://doi.org/10.1080/00380768.2014.919834.

Salehi Lisar, S.Y., Motafakkerazad, R., Rahm, I.M. (2012). Water stress in plants: causes, effects and responses. *Water Stress*, *January*. doi: 10.5772/39363.

Sangeetha, K., Pradeeba, S.S., Santhosh, A., Selvamani, T., 2019. Paddy monitoring and management system. Int. J. Appl. Eng. Res. 14 (5), 1045–1048.

Sharil, S., Wan Mohtar, W.H.M., Mohd Razali, S.F., 2016. Characteristics of flow through rigid, emergent and sparse vegetation. J. Teknol. 78 (10), 77–85. https://doi.org/10.11113/jt.v78.6506.

Shereen, A., Mumtaz, S., Raza, S., Khan, M.A., Solangi, S., 2005. Salinity effects on seedling growth and yield components of different inbred rice lines. Pak. J. Bot. 37 (1), 131–139.

Shi, T., Liu, H., Chen, Y., Wang, J., Wu, G., 2016. Estimation of arsenic in agricultural soils using hyperspectral vegetation indices of rice. J. Hazard. Mater. 308, 243–252. https://doi.org/10.1016/j.jhazmat.2016.01.022.

Singh, H., Singh, R.K. 2016. *Environmental factors affecting growth and productivity of*. *November*. doi: 10.13140/RG.2.2.16576.58882.

Wang, F.-M., Huang, J., Tang, Y., Wang, X., 2007. New vegetation index and its application in estimating leaf area index of Rice. Rice Sci. 14 (3), 195–203. https://doi.org/10.1016/s1672-6308(07)60027-4.

Xie, Q., Dash, J., Huang, W., Peng, D., Qin, Q., Mortimer, H., Casa, R., Pignatti, S., Laneve, G., Pascucci, S., Dong, Y., Ye, H., 2018. Vegetation indices combining the red and red-edge spectral information for leaf area index retrieval. IEEE J. Sel. Top. Appl. Earth Obs. Remote Sens. 11 (5), 1482–1492. https://doi.org/10.1109/JSTARS.2018.2813281.

Xu, X., Gu, X., Song, X., Li, C., Huang, W., 2011. Assessing rice chlorophyll content with vegetation indices from hyperspectral data. IFIP Adv. Inf. Commun. Technol. 344 AICT (PART 1), 296–303. https://doi.org/10.1007/978-3-642-18333-1_35.

Yebra, M., Van Dijk, A., Leuning, R., Huete, A., Guerschman, J.P., 2013. Evaluation of optical remote sensing to estimate actual evapotranspiration and canopy conductance. Remote Sens. Environ. 129, 250–261. https://doi.org/10.1016/j.rse.2012.11.004.

Yeom, J., Jung, J., Chang, A., Ashapure, A., Maeda, M., Maeda, A., Landivar, J., 2019. Comparison of vegetation indices derived from UAV data for differentiation of tillage effects in agriculture. Remote Sens. (Basel) 11 (13). https://doi.org/10.3390/rs11131548.

Zaitunah, A., Samsuri, Ahmad, A.G., Safitri, R.A. 2018. Normalized difference vegetation index (ndvi) analysis for land cover types using Landsat 8 oil in Besitang watershed Indonesia. *IOP Conf. Series: Earth Environ. Sci.*, *126*(012112). doi: doi:10.1088/1755-1315/126/1/012112.

Zhang, C., Kovacs, J.M., 2012. The application of small unmanned aerial systems for precision agriculture: A review. Precis. Agric. 13 (6), 693–712. https://doi.org/10.1007/s11119-012-9274-5.